Biomaterials 32 (2011) 3413–3422

Contents lists available at ScienceDirect

Biomaterials

journal homepage: www.elsevier.com/locate/biomaterials

Engineering spatial control of multiple differentiation fates within a stem cell population

Elmer D.F. Ker [a,d], Bur Chu [b,d], Julie A. Phillippi [e], Burhan Gharaibeh [f], Johnny Huard [f], Lee E. Weiss [c,d], Phil G. Campbell [a,b,d,*]

[a] Department of Biological Sciences, Carnegie Mellon University, 4400 Fifth Avenue, Pittsburgh, PA 15213, USA
[b] Department of Biomedical Engineering, Carnegie Mellon University, 5000 Forbes Avenue, Pittsburgh, PA 15213, USA
[c] Robotics Institute, Carnegie Mellon University, 5000 Forbes Avenue, Pittsburgh, PA 15213, USA
[d] Institute for Complex Engineered Systems, Carnegie Mellon University, 1213 Hamburg Hall, 5000 Forbes Avenue, Pittsburgh, PA 15213, USA
[e] University of Pittsburgh, Thomas E. Starzl Biomedical Science Tower, Department of Surgery, PA 15260, USA
[f] Stem Cell Research Centre of Children's Hospital, UPMC, Bridgeside Point II Bldg, Suite 206 450 Technology Drive, Pittsburgh, PA 15219, USA

ARTICLE INFO

Article history:
Received 31 December 2010
Accepted 13 January 2011
Available online 12 February 2011

Keywords:
Bone
BMP (bone morphogenetic protein)
ECM (extracellular matrix)
Fibroblast growth factor
Muscle
Tendon

ABSTRACT

The capability to engineer microenvironmental cues to direct a stem cell population toward multiple fates, simultaneously, in spatially defined regions is important for understanding the maintenance and repair of multi-tissue units. We have previously developed an inkjet-based bioprinter to create patterns of solid-phase growth factors (GFs) immobilized to an extracellular matrix (ECM) substrate, and applied this approach to drive muscle-derived stem cells toward osteoblasts 'on-pattern' and myocytes 'off-pattern' simultaneously. Here this technology is extended to spatially control osteoblast, tenocyte and myocyte differentiation simultaneously. Utilizing immunofluorescence staining to identify tendon-promoting GFs, fibroblast growth factor-2 (FGF-2) was shown to upregulate the tendon marker Scleraxis (Scx) in C3H10T1/2 mesenchymal fibroblasts, C2C12 myoblasts and primary muscle-derived stem cells, while downregulating the myofibroblast marker α-smooth muscle actin (α-SMA). Quantitative PCR studies indicated that FGF-2 may direct stem cells toward a tendon fate via the *Ets* family members of transcription factors such as *pea3* and *erm*. Neighboring patterns of FGF-2 and bone morphogenetic protein-2 (BMP-2) printed onto a single fibrin-coated coverslip upregulated Scx and the osteoblast marker ALP, respectively, while non-printed regions showed spontaneous myotube differentiation. This work illustrates spatial control of multi-phenotype differentiation and may have potential in the regeneration of multi-tissue units.

1. Introduction

The musculoskeletal system comprises multiple tissue types including bone, muscle, tendon, ligament and cartilage as well as their respective tissue interfaces such as bone-to-tendon entheses and muscle-to-tendon junctions. The maintenance and repair of these multi-tissue structures involves the spatial control of stem cell differentiation toward tissue-specific cells, such as osteoblasts, tenocytes and myocytes [1]. This process is regulated by physical and biochemical microenvironmental cues imparted by the interactions of cells with their extracellular matrix (ECM), neighboring cells, and secreted local and systemic signaling molecules, including growth factors (GFs) [1,2]. Signaling molecules, regulate the pericellular environment where they reside in both the 'liquid-phase' (freely diffusing) form and the 'solid-phase' (immobilized) form that exists in an equilibrium state between desorption from and adsorption to the ECM and cell surfaces [3]. The unique architecture and biochemical composition of the ECM allows it to sequester (immobilize) and release GFs at picogram to nanogram levels [3–7], and can negatively or positively regulate GF bioactivity and bioavailability [3]. As such, GF sequestration by the ECM immobilizes GFs to specific locations, which in turn imparts the temporal and spatial cues required for directing cell behaviors such as cell adhesion, migration, proliferation, differentiation and apoptosis, which are vital for orchestrating complex processes such as development, maintenance and wound healing [3,7–19]. Therefore, developing toolsets that can be used to selectively control the physical placement and dosage of multiple exogenous

* Corresponding author. Institute for Complex Engineered Systems, Carnegie Mellon University, 1213 Hamburg Hall, 5000 Forbes Avenue, Pittsburgh, PA 15213, USA. Tel.: +1 412 268 4126; fax: +1 412 268 5229.
E-mail address: pcampbel@cs.cmu.edu (P.G. Campbell).

0142-9612/$ – see front matter © 2011 Elsevier Ltd. All rights reserved.
doi:10.1016/j.biomaterials.2011.01.036

GFs in a physiologically-relevant manner in order to spatially direct a stem cell population toward multiple cell fates simultaneously is a logical consideration for studying stem cell behaviors and may also have direct applications in regenerative medicine.

Prior work reported by our group and by others has shown that ECMs patterned with solid-phase GFs can be engineered to control various aspects of stem cell behavior, including proliferation, migration and differentiation *in vitro* [8,13,14,16,20–23] as well as differentiation *in vivo* [10]. We previously demonstrated that a GF-patterned fibrin ECM created using an inkjet-based bioprinting technology can drive a single stem cell population toward osteoblast and myocyte fates simultaneously, in registration to printed patterns *in vitro* [16]. In the work presented here, we report on the extension of this approach to spatially drive stem cell differentiation toward a tendon fate simultaneously with osteoblast and myocyte differentiation.

Using solid-phase GFs to direct stem cells to tenocytes *in vitro* has not been previously reported in literature. Therefore, prior to studying multi-lineage patterning, candidate tendon-promoting GFs had to be identified and validated. Candidate GFs were screened against mouse C3H10T1/2 mesenchymal fibroblasts, C2C12 myoblasts and primary muscle-derived stem cells (MDSCs) using both liquid- and solid-phase immunofluorescence staining for the tendon marker Scleraxis (Scx) [24,25]. Quantitative PCR studies were subsequently performed to elucidate the mechanism by which stem cells differentiated toward a tendon lineage. Following this, solid-phase presentation of FGF-2 and/or BMP-2 on fibrin-coated glass coverslips using either coarse hand-printing or high resolution, low-dose inkjet bioprinting was used to demonstrate spatial control of stem cell differentiation toward multiple cell fates simultaneously.

2. Materials and methods

2.1. Cell culture

Multipotent mouse C3H10T1/2 cells (ATTC, Manassas, VA) were grown in Dulbecco's Modified Eagle's Media (DMEM; Invitrogen, Carlsbad, CA), 10% fetal bovine serum (Invitrogen, Carlsbad, CA) and 1% penicillin-streptomycin (PS; Invitrogen, Carlsbad, CA). Mouse C2C12 cells (ATTC, Manassas, VA) were grown in DMEM, 10% bovine serum (Invitrogen, Carlsbad, CA) and 1% PS. Multipotent MDSCs were isolated from primary mouse gastrocnemius muscle biopsies following a modified preplate technique [26] and were grown in DMEM (high glucose), 10% horse serum (HS; Invitrogen, Carlsbad, CA), 10% FBS, 0.5% Chick Embryo Extract (Accurate Chemical Co, Westbury, NY) as previously described [26,27]. For myogenic differentiation, cells were grown in low serum containing myogenic differentiation (DMEM, 2% HS, 1% PS) media for 3–5 days. This media is subsequently referred to as myogenic media or myogenic conditions for the remainder of the text. All cells were kept at 37 °C, 5% CO_2 in a humidified incubator.

2.2. Growth factor preparation and use

Recombinant human BMP-2 (Genetics Institute Inc, Cambridge, MA), FGF-2 (Peprotech, Rockyhill, NJ), FGF-4 (Peprotech, Rockyhill, NJ) and GDF-7 (Prospc Bio, Rehovot, Israel) were reconstituted according to manufacturer's instructions to 1–2 mg/mL, aliquoted and stored at −80 °C. Prior to use, GFs were freshly diluted to the desired concentration in 10 mM sodium phosphate, pH 7.4. For liquid-phase GF experiments, cells were seeded at 2.6–3.1 $\times 10^4$ cells/cm^2 in the presence or absence of GF (1–500 ng/mL) under proliferation (High serum) and myogenic (Low serum) media for 3–4 days. For solid-phase GF experiments, cells were seeded at 3.1–3.6 $\times 10^4$ cells/cm^2 over printed fibrin-coated coverslips under proliferation and myogenic media for 3–4 days.

2.3. Preparation of fibrin coated coverslips

Homogenous fibrin films were prepared essentially as described by Campbell et al., 2005 [8]. Briefly, 18 × 18 mm epoxy-silanized glass coverslips (Thermo Fisher Scientific, Waltham, MA) were coated with 0.1 mg/mL fibrinogen (Aventis Behring, King of Prussia, PA or American Diagnostica Inc., Stanford, CT)and converted into fibrin by incubating coverslips in 4 U/mL thrombin (Enzyme Research Laboratories, South Bend, IN). Coverslips were then washed with phosphate buffered saline (PBS) and sterile deionized water before air-drying in a laminar flow hood. The thickness of the fibrin films was previously estimated to be approximately 20 nm [8].

2.4. Growth factor printing

Prior to printing, GFs were freshly diluted to the desired concentration in 10 mM sodium phosphate, pH 7.4. Prior to filling the inkjet with the GF, the printhead was sterilized by rinsing with 70% ethanol followed by sterile deionized water. The bio-ink, consisting of 100–200 μg/ml GF was loaded into the printhead, and printed onto fibrin-coated glass coverslips as previously described [8,14]. The concentration of inkjetted GFs can be modulated by overprinting, which is achieved by varying the number of times a GF is deposited in the same (x,y) location. In the case of hand-printed GF patterns, 1–2 μL of a 100 μg/mL GF solution was pipetted onto a fibrin-coated glass coverslip instead and a diamond scribe pen was used to mark the droplet perimeter after it had been allowed to air-dry for 1 h at 37 °C. After printing, fibrin-coated coverslips were incubated in PBS for 5 min followed by serum-free DMEM with 1% PS overnight at 37 °C, 5% CO_2 to wash off unbound GF prior to cell seeding. The surface concentration of GF present on fibrin-coated coverslips during cell seeding was estimated based on desorption measurements in previous studies [8,13,14,28].

2.5. Quantitative PCR

For the experiments investigating Scx expression during muscle differentiation, C2C12 cells were grown at 1.55 $\times 10^2$ cells/cm^2 under proliferation conditions and at 2.5 $\times 10^3$ cells/cm^2 under myogenic conditions for 4 days to ensure similar number of cells in both conditions prior to RNA extraction. C3H10T1/2 cells were grown in proliferation medium at 1.5–2.0 $\times 10^4$ cells/cm^2 in the presence or absence of FGF-2 (50 μg/mL) for 36 h and 72 h prior to extraction of total RNA (RNeasy Mini Kit; Qiagen, Valencia, CA). Quantitative polymerase chain reaction analysis for *pea3*, *erm* and Scx were performed as previously described [29,30]. Target gene expression was normalized to 18S internal control. Gene expression is displayed as the mean of five independent experiments and represented as mean ± Standard Error Mean (SEM). Statistical analysis was performed as described below.

2.6. Immunofluorescence staining

Cells were washed in PBS, fixed in methanol for 5 min, air-dried and blocked with 10% donkey serum (Jackson Immunoresearch, West Gove, PA) for 20 min at RT. For mouse-on-mouse staining, an additional blocking step was performed by incubating cells with 100 μg/mL donkey anti-mouse FAB (Jackson Immunoresearch, West Gove, PA) for 1 h at RT. Cells were then rinsed with wash buffer (PBS, 0.1%BSA) and incubated with primary antibodies: rabbit anti-Scx (10 μg/mL; Abcam, Cambridge, MA), mouse anti-myosin MF20 (1 μg/mL; DSHB, Iowa City, Iowa), mouse anti-α-smooth muscle actin (α-SMA; 1 μg/mL; Abcam, Cambridge, MA) or goat anti-myogenin (2 μg/mL; Santa Cruz Biotechnology Inc, Santa Cruz, CA) overnight at 4 °C. Cells were then rinsed three times with wash buffer and incubated with secondary antibodies for 1 h at RT – donkey anti-goat FITC (4 μg/mL; Santa Cruz Biotechnology Inc, Santa Cruz, CA), donkey anti-mouse Dylight 488 nm or donkey anti-rabbit Dylight 549 nm (15 μg/mL each; Jackson Immunoresearch, West Gove, PA). Lastly, cells were rinsed five times with wash buffer and imaged using a Zeiss Axiovert 200M microscope (Carl Zeiss Microimaging, Thornwood, NY) equipped with a Colibri LED light source. Quantification of immunofluorescence staining was performed using Adobe Photoshop 7.0 (Adobe Systems, San Jose, CA). Briefly, the rectangular marquee tool was used to draw a bounding box (Approximately 700 pixels by 700 pixels representing an area 0.9 mm by 0.9 mm in size) and the image histogram tool was used to measure average pixel intensity. Statistical analysis was performed as described below.

2.7. ALP stain

Cells were seeded onto GF patterns for 72 h, washed in PBS and fixed for 2 min in 3.7% formaldehyde. Alkaline phosphatase activity (ALP; SIGMAFAST) was detected according to the manufacturer's instructions (Sigma–Aldrich, St. Louis, MO). Where required, alkaline phosphatase-stained images were converted to CMYK format since this color format is representative of reflected light colors as opposed to emitted light colors (RGB). Since cyan and magenta form the color blue, these channels were added together and inverted. The average pixel intensity was determined using the image histogram tool in Adobe Photoshop 7.0 (Adobe Systems, San Jose, CA).

2.8. Statistical analysis

For both quantitative PCR and immunofluorescence analysis, one-way analysis of variance followed by Fisher's least significant difference post hoc test using SYSTAT 9 software (Systat Software Inc., Richmond, CA) was performed to determine significance among treatment groups. A p value ≤ 0.05 was considered statistically significant.

3. Results

3.1. Effect of liquid-phase FGF-2 and FGF-4 on Scx expression in C3H10T1/2 cells

Liquid-phase experiments incorporating a combination of 200 ng/mL BMP-2, 500 ng/mL BMP-12/GDF-7 and 50 ng/mL FGF-2 indicated that C3H10T1/2 cells upregulated the tendon marker Scx in the presence of FGF-2 alone but not with GDF-7 or BMP-2 (Supplementary Fig. 1). In addition, FGF-2-treated cells adopted an elongated spindle-like morphology reminiscent of tenocytes (Supplementary Fig. 1). When treated with 50 ng/mL FGF-4, C3H10T1/2 cells showed punctate nuclear staining of Scx transcription factor (Supplementary Fig. 2).

3.2. Effect of liquid-phase FGF-2 on Scx expression in C2C12 cells

Scx expression in C2C12 cells was examined under proliferation (high serum) as well as myogenic (low serum) conditions to determine if such cells could undergo tendon specification when treated with FGF-2. Under proliferation conditions, increasing amounts of FGF-2 resulted in upregulation of the tendon marker Scx in a dose-dependent manner with punctate nuclear staining of Scx observed in cells treated at 25 ng/mL FGF-2 and 50 ng/mL FGF-2 (Supplementary Fig. 3). Under myogenic conditions, Scx expression was unexpectedly upregulated in nascent myotubes in the absence of FGF-2 (Supplementary Fig. 4). Confocal sectioning studies determined that the thickness of myotubes, which is observed as a bright halo around cells in phase-contrast images (Supplementary Fig. 4), contributed in part to the high levels of Scx (data not shown). Furthermore, quantitative PCR analysis indicated that there was no fold change in Scx expression between proliferating C2C12 cells (1.003 ± 0.075 fold change) and differentiating myotubes (1.022 ± 0.209 fold change). In the presence of FGF-2, myotube formation was inhibited and cells showed increased Scx expression when compared to non-myocytes in untreated control (Supplementary Fig. 4).

3.3. Effect of liquid-phase FGF-2 on Scx expression in MDSCs

Tendon specification in MDSCs was examined in cells treated with FGF-2 under proliferation and myogenic conditions. Under proliferation conditions, FGF-2 dose-dependently increased expression of the tendon marker Scx with punctate nuclear staining of Scx occasionally observed at 50 ng/mL FGF-2 (Fig. 1). Similar to C2C12 cells, Scx expression was upregulated in nascent myotubes in the absence of FGF-2. In the presence of FGF-2, myotube formation was inhibited with MDSCs exhibiting lower levels of the myogenic marker myogenin (Supplementary Fig. 5). In addition, Scx expression was upregulated when compared to non-myocytes in untreated control and FGF-2-treated cells did not show increased expression for the myofibroblast marker α-smooth muscle actin (α-SMA; Supplementary Fig. 6).

3.4. Regulation of Scx in C3H10T1/2 cells

As previous studies indicated that members of the *Ets* family of transcription factors such as *pea3* and *erm* were involved in regulation of Scx during tendon development in the chick, quantitative PCR analysis of these genes were performed to determine if a similar mechanism was operating in these stem cell populations [31]. 50 ng/mL FGF-2 upregulated *pea3* (43.1 ± 27.5 fold change, $p = 0.005$) and *erm* (16.5 ± 6.5 fold change, $p = 0.178$) at 36 h whereas Scx levels remained constant. At 72 h, all three genes were upregulated: *pea3* (169.6 ± 45.8 fold change, $p = 0.008$), *erm* (72.5 ± 16.2 fold change, $p = 0.033$) and Scx (22.8 ± 5.4 fold change, $p = 0.006$). As such, the prior induction of *pea3* and *erm* suggest that these two genes lie upstream of Scx (Fig. 2).

3.5. Effect of solid-phase FGF-2 on Scx expression in C3H10T1/2 cells

Having demonstrated that Scx expression was upregulated by liquid-phase FGFs, square patterns of FGF-2 (each measuring 1 by 1 mm) were inkjet printed onto fibrin-coated glass coverslips with 2, 6 and 12 overprints to determine if solid-phase GF patterns can spatially direct tendon specification in a dose-dependent manner. Our previous studies have shown that the surface concentration of GF that is deposited can be modulated by overprinting and that such GF patterns can persist for up to 144 h under standard cell culture conditions [10,13,14,16]. As shown in Fig. 3A, the amount of FGF-2 deposited in 2, 6 and 12 overprints after washing and prior to cell seeding was estimated to be 40.8 pg/mm^2, 122.4 pg/mm^2 and 244.8 pg/mm^2 FGF-2 based on previous studies [8,13,14,28]. Under proliferation conditions (High serum), C3H10T1/2 cells showed upregulation of Scx in response to solid-phase patterning of FGF-2 in a dose-dependent manner (Fig. 3B). Although the lowest dose of solid-phase FGF-2 (40.8 pg/mm^2) was not sufficient to induce an increase in Scx expression relative to negative control/non-printed regions ($p = 0.872$), higher doses of solid-phase FGF-2 resulted in an increase in Scx expression relative to negative control/non-printed regions ($p = 0.009$ for 122.4 pg/mm^2 FGF-2 and $p = 0.001$ for 244.8 pg/mm^2 FGF-2; Fig. 3) in C3H10T1/2 cells. Thus, solid-phase patterning of FGF-2 can spatially control tendon cell fate (Fig. 3).

3.6. Effect of solid-phase FGF-2 on MF20 and Scx expression in C2C12 cells

Similarly, square patterns of FGF-2 (each measuring 1 by 1 mm) were inkjet printed onto fibrin-coated glass coverslips with 5, 10 and 30 overprints (corresponding to an estimated amount of 102 pg/mm^2, 203 pg/mm^2 and 612 pg/mm^2 FGF-2) to determine if multiple stem cell fates could be spatially controlled in a dose-dependent manner within the same construct. Under both proliferation and myogenic conditions, inkjet printed patterns of FGF-2 resulted in a dose-dependent increase in Scx expression (Fig. 4B, C).

Under proliferation conditions, although the lowest dose of solid-phase FGF-2 (102 pg/mm^2 FGF-2) was not sufficient to induce an increase in Scx expression relative to negative control/non-printed regions ($p = 0.099$), higher doses of solid-phase FGF-2 resulted in an increase in Scx expression relative to negative control/non-printed regions ($p = 0.01$ for 203 pg/mm^2 FGF-2 and $p = 0.000$ for 612 pg/mm^2 FGF-2) in C2C12 cells (Fig. 4C). Under myogenic conditions, although lower doses of solid-phase FGF-2 were not sufficient to induce an increase in Scx expression relative to negative control/non-printed regions ($p = 0.139$ for 102 pg/mm^2 FGF-2 and $p = 0.053$ for 203 pg/mm^2 FGF-2), the highest dose of solid-phase FGF-2 resulted in an increase in Scx expression relative to negative control/non-printed regions ($p = 0.022$ for 612 pg/mm^2 FGF-2) in C2C12 cells (Fig. 4C). Within and outside the printed regions, cells fused to form multinucleated myotubes as a result of high cell density leading to spontaneous cell fusion under proliferation conditions or direct myogenic induction, as evidenced by the presence of muscle myosin or MF20 (Fig. 4B). No difference in MF20 staining was observed between printed and non-printed regions ($p > 0.05$ for all cases). Taken together, these results demonstrate the simultaneous specification of myocyte and tenocyte fates within the same construct in a spatially defined manner in a dose-dependent fashion.

3.7. Effect of solid-phase BMP-2 and FGF-2 on ALP, MF20 and Scx expression in C2C12 cells

Having demonstrated that multiple stem cell fates could be spatially controlled within the same construct, inkjet bioprinting

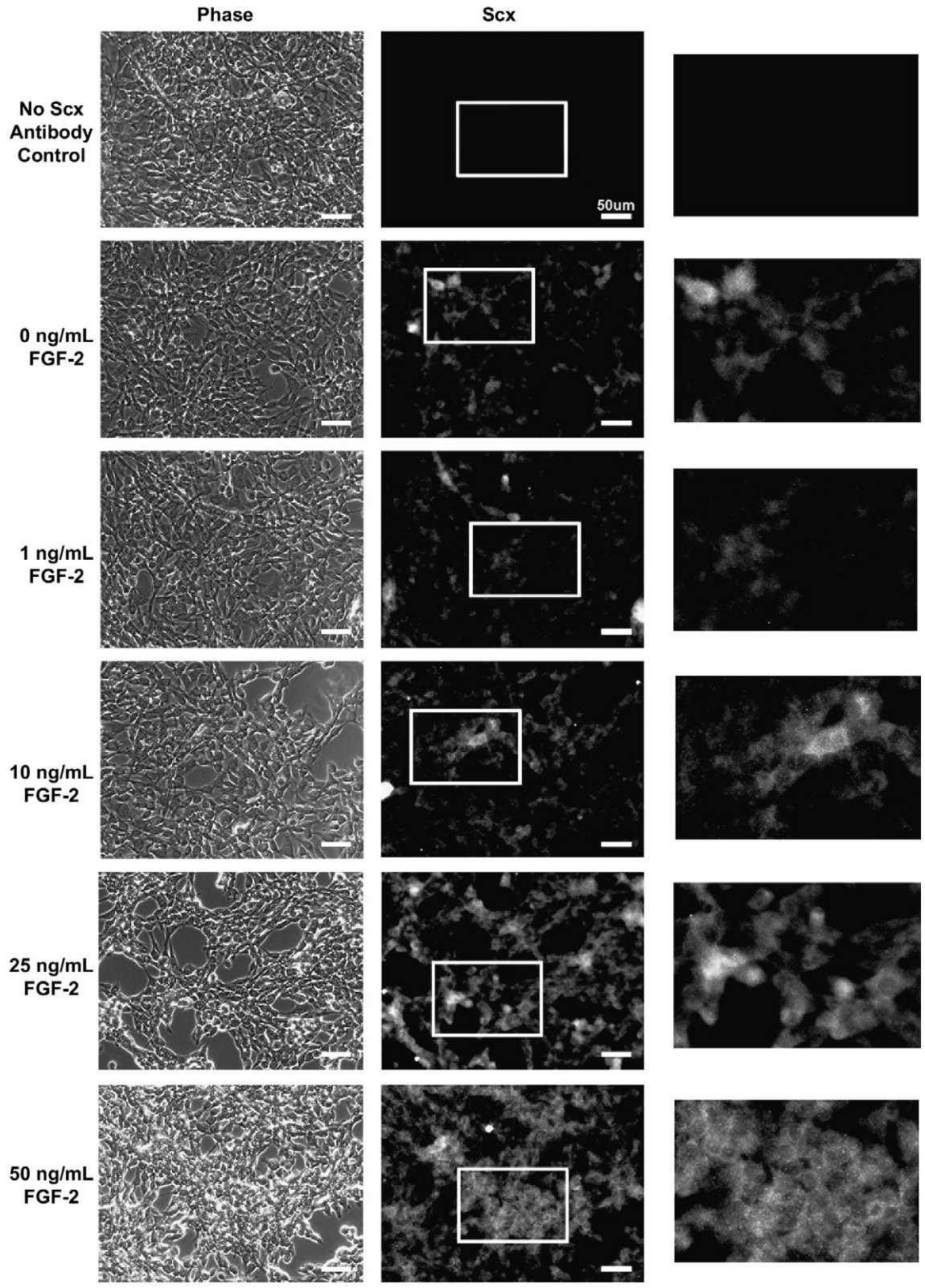

Fig. 1. Dose-dependent effect of FGF-2 on expression of tendon marker Scx in mouse MDSCs after 72 h in proliferation media. Increasing amounts of FGF-2 resulted in upregulation of tendon marker Scx. White box indicates magnified region (right). Note the punctate nuclear staining of Scx transcription factor in 50 ng/ml FGF-2. Scale bar 50 μm.

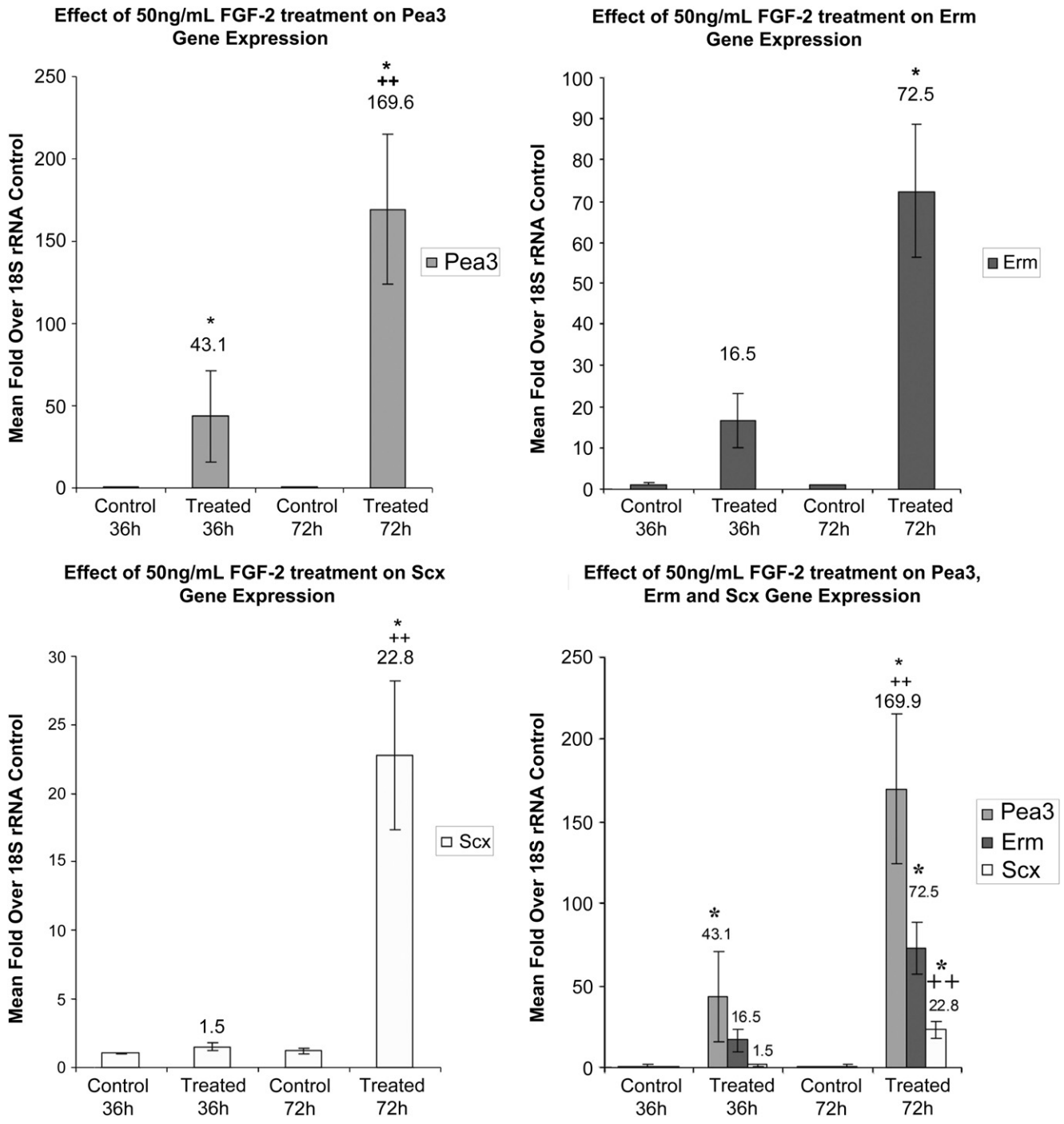

Fig. 2. Effect of 50 ng/mL FGF-2 on expression of *pea3*, *erm* and Scx transcription factors in mouse C3H10T1/2 cells at 36 h and 72 h in proliferation media. At 36 h, FGF-2 increased *pea3* and *erm* but not *Scx* expression, relative to control. At 72 h, all transcription factors are upregulated, relative to control. Columns indicate fold changes over control ± SEM ($n = 5$). *, Significantly different from control; $p \leq 0.05$. + +, Significantly different from 36 h; $p \leq 0.05$.

technology was applied to determine if osteoblast, tenocyte and myocyte fates, representative of a primitive bone-tendon-muscle unit, could be simultaneously specified within the same construct. After 72 h in proliferation media, inkjet printed patterns of BMP-2 and FGF-2 increased ALP and Scx expression, respectively (Fig. 5). On inkjet printed patterns of BMP-2, ALP expression was increased relative to negative control/non-printed regions ($p = 0.000$) and inkjet printed patterns of FGF-2 ($p = 0.000$) but no increase in Scx expression was observed relative to negative control/non-printed regions ($p = 0.146$). On inkjet printed patterns of FGF-2, Scx expression was increased relative to negative control/non-printed regions ($p = 0.000$) and inkjet printed patterns of BMP-2 ($p = 0.003$) but no increase in ALP expression was observed relative to negative control/non-printed regions ($p = 0.887$). Within and outside the printed regions, myotube formation was promoted due to the high density of cells resulting in spontaneous fusion of cells (Fig. 5B). No difference in MF20 staining was observed between printed and non-printed regions ($p > 0.05$ for all cases). Taken together, these results demonstrate the simultaneous specification of osteoblast, tenocyte and myocyte fates within the same construct in a spatially defined manner.

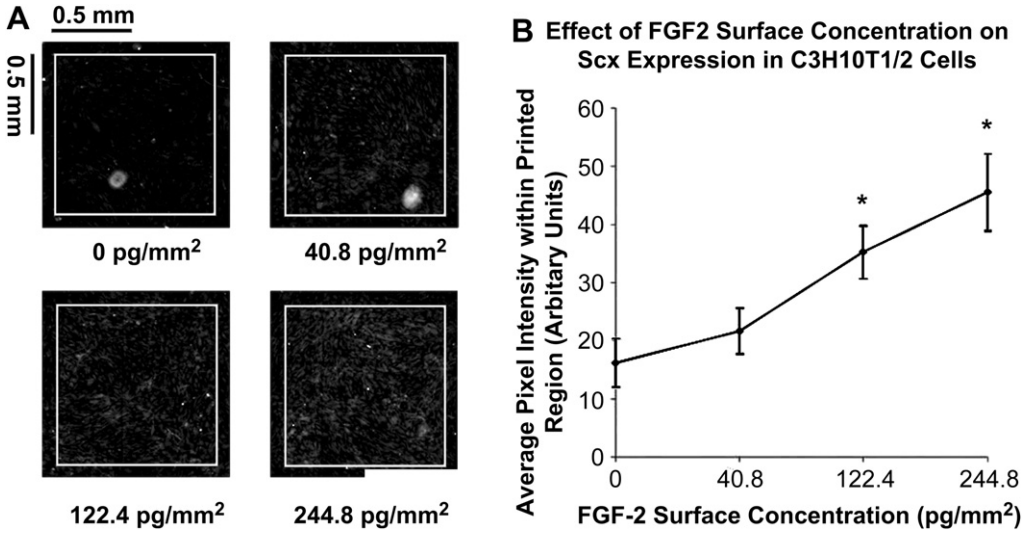

Fig. 3. Effect of inkjet printed patterns of FGF-2 on expression of tendon marker Scx in mouse C3H10T1/2 cells after 72 h in proliferation media. A. Inkjet printed patterns of FGF-2 resulted in upregulation of the tendon marker Scx in a dose-dependent manner. B. Quantification of Scx Expression ($n = 6$). White squares indicates inkjet printed regions. The estimated surface concentration of FGF-2 present during cell seeding (after washing) is shown in terms of picograms/mm^2. Scale bar 500 μm *, Significantly different from control or non-printed regions; $p \leq 0.05$.

3.8. *Effect of solid-phase FGF-2 on α-smooth muscle actin expression in C2C12 cells*

To rule out the possibility that FGF-2 was directing C2C12 cells toward a myofibroblast fate as opposed to a tenocyte fate, FGF-2 was hand-printed onto a fibrin-coated coverslip and immunostained for the myofibroblast marker α-SMA (Fig. 6). After 72 h in proliferation media, α-SMA, which is transiently expressed during muscle differentiation [32], was downregulated on hand-printed patterns of FGF-2, indicating that these cells were differentiating toward a tenocyte fate as opposed to a myofibroblast fate.

4. Discussion

4.1. *Directing osteoblast differentiation*

We previously used our printing approach to demonstrate spatial control of adjacent regions of osteoblast-myocyte differentiation

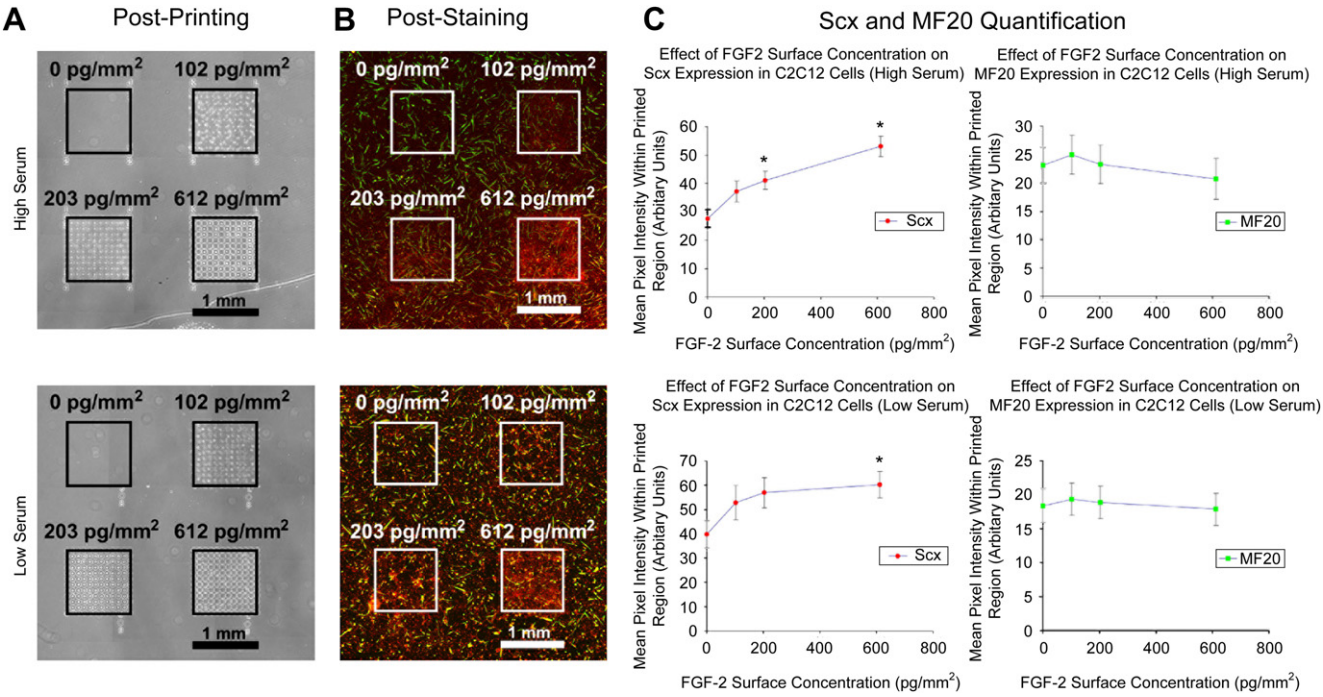

Fig. 4. Effect of inkjet printed patterns of FGF-2 on expression of tendon marker Scx (red) and muscle marker MF20 (green) in mouse C2C12 cells after 72 h in proliferation and myogenic media. Increasing amounts of FGF-2 dose-dependently upregulated Scx and inhibited myotube formation slightly. Non-printed regions showed spontaneous myotube differentiation due to high confluency levels. A. Inkjet printed patterns of FGF-2 (Black squares). B. Scx and MF20 staining of printed patterns (White Squares). C. Quantification of Scx and MF20 stain. The estimated surface concentration of FGF-2 present during cell seeding (after washing) is shown in terms of picograms/mm^2. Scale bar 1 mm. Error bars indicate Standard Error Mean or SEM ($n = 12$ for proliferation media, $n = 16$ for myogenic media). *, Significantly different from control or non-printed regions; $p \leq 0.05$.

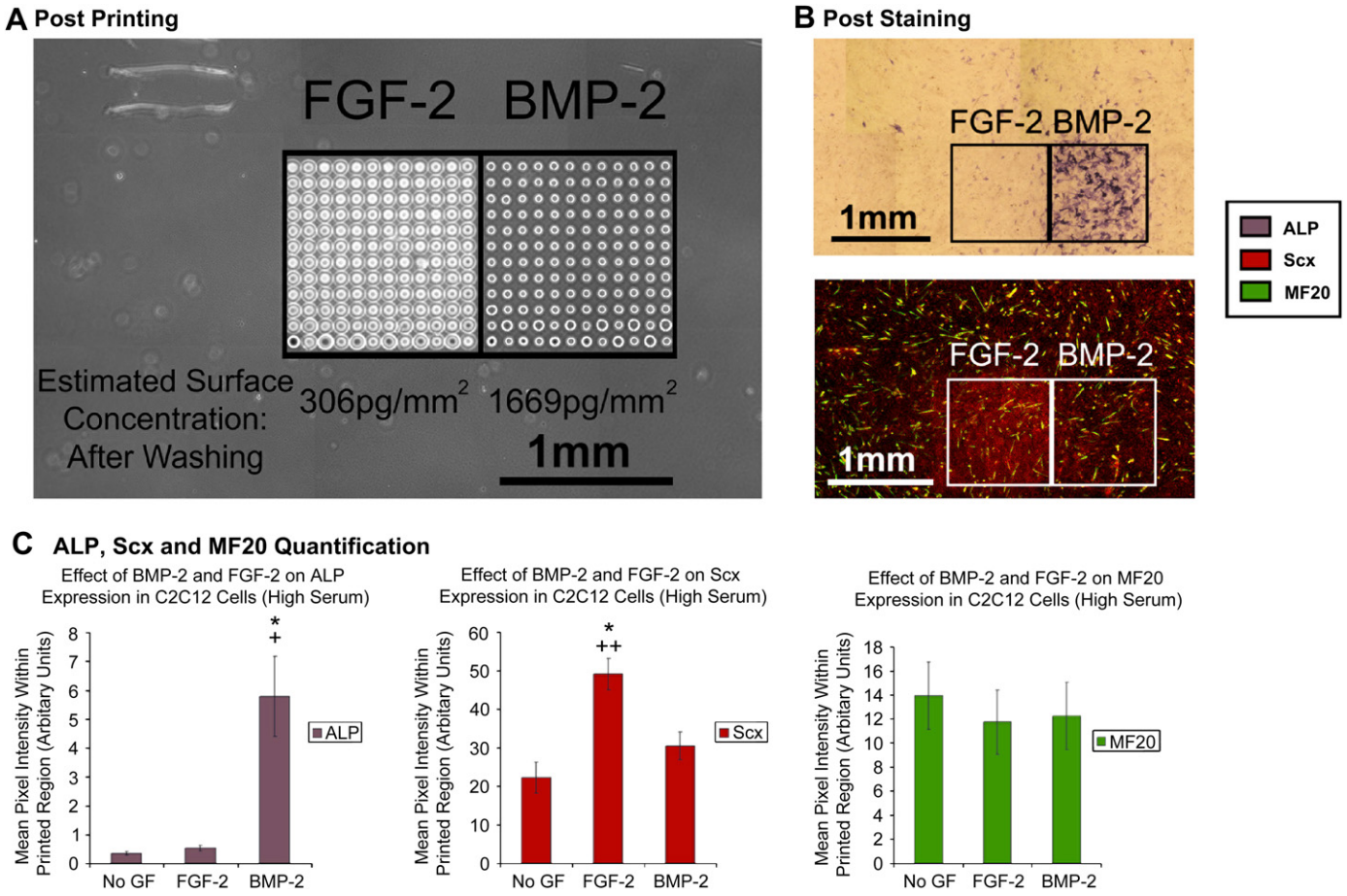

Fig. 5. Effect of inkjet printed patterns of BMP-2 and FGF-2 on expression of osteoblast marker ALP (blue), tendon marker Scx (red) and muscle marker MF20 (green) in mouse C2C12 cells after 72 h in proliferation media. BMP-2 and FGF-2 patterns induced ALP and Scx expression, respectively, while non-printed regions spontaneously formed myotubes. A. Inkjet printed patterns of BMP-2 and FGF-2 (Black squares). B. ALP, Scx and MF20 staining of printed patterns (Black and white squares). C. Quantification of ALP, Scx and MF20 stain. Squares indicates inkjet printed region post-printing or post-immunofluorescence staining. The estimated surface concentration of GF present during cell seeding (after washing) is shown in terms of picograms/mm^2. Scale bar 1 mm. Error bars indicate Standard Error Mean or SEM ($n = 8$). *, Significantly different from control or non-printed regions; $p \leq 0.05$. +, Significantly different from inkjet printed patterns of FGF-2; $p \leq 0.05$. + +, Significantly different from inkjet printed patterns of BMP-2; $p \leq 0.05$.

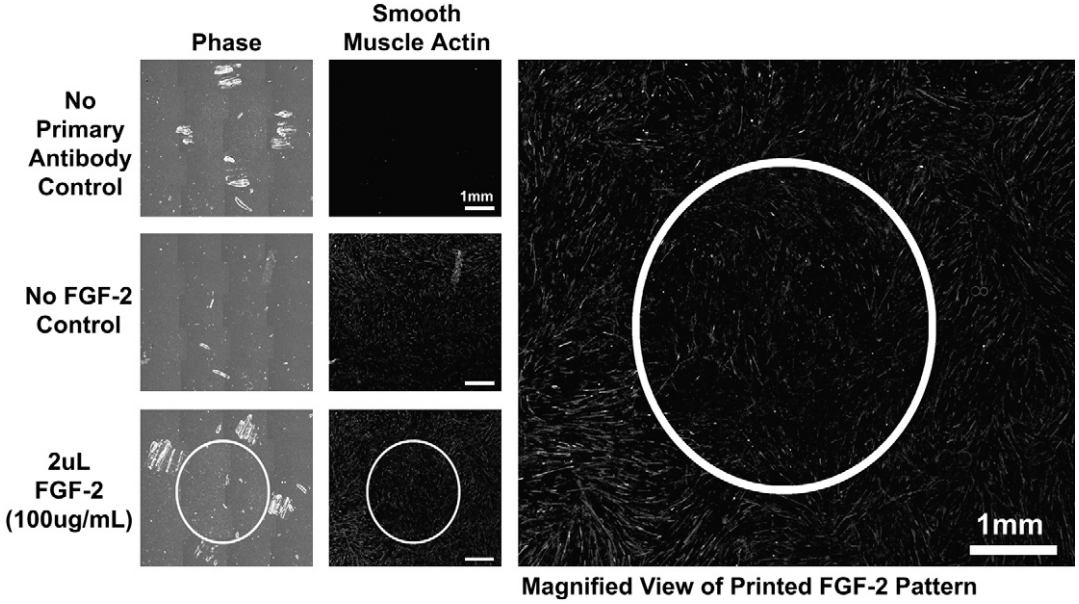

Fig. 6. Effect of FGF-2 on expression of myofibroblast marker α-Smooth Muscle Actin (α-SMA) in mouse C2C12 cells after 72 h in proliferation media. α-SMA expression was downregulated on hand-printed patterns of FGF-2. Parallel lines observed in phase-contrast images denote scratch marks used for identifying the location of hand-printed FGF-2 patterns. White circle indicates the boundary of the hand-printed FGF-2 pattern. Scale bar 1000 μm.

[16]. In particular, when C2C12 cells and MDSCs were cultured under myogenic conditions on BMP-2 patterns printed on fibrin, cells 'on-pattern' differentiated toward the osteoblast lineage, whereas cells 'off-pattern' differentiated toward the myogenic lineage. The purpose of the research reported here was to extend our prior work to the control of more complex osteoblast-tenocyte-myocyte units, representing primitive but physiologically-relevant [33,34] constructs.

4.2. Directing myocyte differentiation

In our original osteoblast-myocyte patterning experiments [16], osteoblasts were explicitly induced 'on-pattern' with solid-phase BMP-2, while myocytes were implicitly induced 'off-pattern' using myogenic media. In an effort to explicitly pattern myocytes for this current study, we investigated numerous GFs and signaling molecules implicated in muscle differentiation, including amphoterin/HMGB1, decorin, follistatin, ghrelin, galectin-1, interleukin-4, insulin-like growth factor-1, insulin-like growth factor-2, neuregulin-1 beta 2, sonic hedgehog and wnt3A [7,35–45]. However, these candidate muscle-promoting cues did not elicit an increased myogenic response relative to control under proliferation conditions in either liquid- or solid-phase experiments (Data not shown). Therefore, we continued to rely on implicit patterning of myocytes off-pattern using either myogenic conditions to induce myogenic differentiation through serum starvation or proliferation conditions to increase cell–cell contact via cell receptors such as N-dherins, leading to spontaneous cell fusion and myotube formation [46,47].

4.3. Directing tenocyte differentiation

There have been no prior reports on the use of solid-phase GFs to direct stem cells toward tenocytes *in vitro*. Furthermore, even liquid-phase protocols for differentiating these cell types to a tendon fate have yet to be firmly established. Since previous studies demonstrated that members of the BMP and FGF family of signaling proteins may be involved in tendon formation [31,48–50], we first screened FGF-2, FGF-4, BMP-2 and BMP-12/GDF-7 in liquid-phase experiments using immunofluorescence staining for the tendon marker Scx [24] to determine if these GFs could direct multipotent stem cells toward a tendon cell fate. Only FGF-2 and FGF-4 in liquid-phase forms were shown to direct C3H10T1/2 cells, C2C12 cells and MDSCs toward a tendon lineage (Supplementary Fig. 1–5 and Fig. 1). To rule out the possibility that FGF-2-treated cells were differentiating toward myofibroblasts as opposed to tenocytes, FGF-2-treated cells were stained for the myofibroblast marker α-SMA. In these studies, FGF-2-treated cells did not induce upregulation of α-SMA in either C2C12 cells or MDSCs, and in fact, reduced expression of α-SMA slightly (Fig. 6 and Supplementary Fig. 6). Quantitative PCR analysis subsequently determined that the mechanism by which these stem cells differentiate toward a tendon fate may involve members of the *Ets* family of transcription factors such as *pea3* and *erm*, which may act upstream of the tendon transcription factor Scx (Fig. 2), a finding that parallels tendon development in chick [31].

Unexpectedly, high levels of Scx expression were observed in nascent myotubes (Supplementary Figs. 4 and 5). This was later shown to be contributed, in part, by the thickness of myotubes, as evidenced by the bright halo around cells in phase-contrast images (Supplementary Figs. 4 and 5) and confocal sectioning studies (data not shown). In addition, there was no change in Scx gene expression during myogenesis although increased levels of Scx protein in myotubes could be accounted for by post-transcriptional processes. Alternatively, myotubes may show increased Scx levels since Scx is a transcription factor that lies upstream of collagen, a major non-contractile component of muscle. However, this is unlikely since nascent myotubes exhibit little to no nuclear staining of Scx when compared to FGF-2-treated cells (Supplementary Figs. 4 and 5).

4.4. Solid-phase patterning of GFs using high resolution, low-dose bioprinting

FGF-2 was used for all subsequent solid-phase tenocyte patterning experiments using high resolution, low-dose inkjet bioprinting because FGF-4 elicted a lower response in hand-printed and qPCR experiments (Data not shown). In these studies, C3H10T1/2 cells were shown to upregulate the tendon marker Scx in a dose-dependent fashion in response to inkjet printed patterns of FGF-2 (Fig. 3). Similarly, C2C12 cells also dose-dependently upregulated the tendon marker Scx in response to inkjet printed patterns of FGF-2, with spontaneous fusion of myotubes occurring predominantly outside the printed region (Fig. 4). Having demonstrated that solid-phase patterning of tenocytes and myocytes can be engineered under proliferation and myogenic conditions within the same construct, adjacent printed patterns of FGF-2 and BMP-2 were tested and shown to specify osteoblasts, tenocytes and myocytes within the same construct, representing a primitive muscle-tendon-bone unit (Fig. 5). Although FGF-2 displays a clear dose-dependence increase on tendon cell differentiation, some variations in cell responses to printed GF patterns were observed. For example, some C2C12 cells that were 'off-pattern' but in close proximity to high doses of FGF-2 or BMP-2 patterns exhibited weak Scx (Fig. 4B, high serum panel) or ALP staining (Fig. 5B), respectively. These variations may stem from desorption of GF from the printed region followed by its readsorption outside the printed region prior to cell seeding or by paracrine signaling from cells 'on-pattern' to cells 'off-pattern' to differentiate. In addition, the differentiation response of cells within a printed GF pattern was not homogenous throughout as shown by non-uniform Scx staining along with sporadic MF20 staining on printed FGF-2 patterns (Figs. 3–5) and uneven ALP staining on printed BMP-2 patterns (Fig. 5). This may be a function of several factors, including: non-uniform GF distribution within the printed region following inkjet printing and GF drying [28]; GF desorption followed by readsorption prior to cell seeding [13,14,51,52]; uneven cell density during cell seeding; cell heterogeneity [53]; or, a combination of all these factors. Furthermore, when multiple GFs are utilized, the dosage of individual GFs was found to be critical for simultaneously specifying multiple cell fates. When similar concentrations of FGF-2 and BMP-2 were inkjet bioprinted in close proximity, no positive ALP staining was observed on printed BMP-2 patterns (Data not shown). This may be attributed to desorption of FGF-2 from the fibrin surface followed by binding to the surface of cells seeded on printed BMP-2 patterns, resulting in the inhibition of BMP-2-induced osteoblast differentiation, which is an effect that is well characterized [14,54]. This problem was eventually resolved by empirically optimizing the amount of BMP-2 and FGF-2 deposited by inkjet bioprinting, resulting in excess surface concentration of BMP-2 to overcome this inhibitory effect (Fig. 5).

This work has demonstrated that inkjet-based bioprinting technology enables the investigation of spatial control of solid-phase GF-directed differentiation of stem cells toward single or multiple fates in physiologically-relevant engineered microenvironments *in vitro*. Our prior work also provides support for the application of this technology *in vivo* [10]. Together, these *in vitro* and *in vivo* studies suggest that this technology may have practical implications for both basic scientific research and therapy development and deployment targeting the musculoskeletal system.

5. Conclusions

This report identified both liquid- and solid-phase FGF-2 as being capable of upregulating the tendon marker Scx in C3H10T1/2 cells, C2C12 cells and MDSCs. Quantitative PCR analysis suggests that members of the *Ets* family of transcription factors such as *pea3* and *erm* may lie upstream of Scx. This report also demonstrates how inkjet bioprinting technology can create persistent GF patterns that direct a single stem cell population toward multiple fates, including tenocytes, myocytes or osteoblasts, within the same construct in a spatially defined manner. This capability not only offers an approach to study multi-lineage differentiation *in vitro*, but may also be translatable to new therapies to treat disease and trauma of the musculoskeletal system.

Acknowledgments

We would like to thank James Fitzpatrick for assistance with fluorescence microscopy and Larry Schultz for assistance with GF printing. This work was supported by NIH grants RO1EB004343 and RO1EB007369 as well as funding from the Pennsylvania Infrastructure Technology Alliance (PITA).

Appendix

Figures with essential color discrimination. Figs. 4 and 5 in this article are difficult to interpret in black and white. The full color images can be found in the on-line version, at doi:10.1016/j.biomaterials.2011.01.036.

Appendix A. Supplementary material

Supplementary data associated with this article can be found, in the online version, at doi:10.1016/j.biomaterials.2011.01.036.

References

[1] Scadden DT. The stem-cell niche as an entity of action. Nature 2006;441(7097):1075–9.
[2] Nelson CM, Bissell MJ. Of extracellular matrix, scaffolds, and signaling: tissue architecture regulates development, homeostasis, and cancer. Annu Rev Cell Dev Biol 2006;22:287–309.
[3] Taipale J, Keski-Oja J. Growth factors in the extracellular matrix. Faseb J 1997;11(1):51–9.
[4] Canalis E. Growth factor control of bone mass. J Cell Biochem 2009;108(4):769–77.
[5] Chen D, Zhao M, Mundy GR. Bone morphogenetic proteins. Growth Factor 2004;22(4):233–41.
[6] Choi YJ, Lee JY, Park JH, Park JB, Suh JS, Choi YS, et al. The identification of a heparin binding domain peptide from bone morphogenetic protein-4 and its role on osteogenesis. Biomaterials 2010;31(28):7226–38.
[7] Unsicker K, Krieglstein K. Cell signaling and growth factors in development. Germany: WILEY-VCH; 2006.
[8] Campbell PG, Miller ED, Fisher GW, Walker LM, Weiss LE. Engineered spatial patterns of FGF-2 immobilized on fibrin direct cell organization. Biomaterials 2005;26(33):6762–70.
[9] Carinci P, Becchetti E, Baroni T, Carinci F, Pezzetti F, Stabellini G, et al. Extracellular matrix and growth factors in the pathogenesis of some craniofacial malformations. Eur J Histochem 2007;51(Suppl. 1):105–15.
[10] Cooper GM, Miller ED, Decesare GE, Usas A, Lensie EL, Bykowski MR, et al. Inkjet-based biopatterning of bone morphogenetic protein-2 to spatially control calvarial bone formation. Tissue Eng Part A 2010;16(5):1749–59.
[11] Datta N, Holtorf HL, Sikavitsas VI, Jansen JA, Mikos AG. Effect of bone extracellular matrix synthesized in vitro on the osteoblastic differentiation of marrow stromal cells. Biomaterials 2005;26(9):971–7.
[12] DeCarlo AA, Whitelock JM. The role of heparan sulfate and perlecan in bone-regenerative procedures. J Dent Res 2006;85(2):122–32.
[13] Miller ED, Fisher GW, Weiss LE, Walker LM, Campbell PG. Dose-dependent cell growth in response to concentration modulated patterns of FGF-2 printed on fibrin. Biomaterials 2006;27(10):2213–21.
[14] Miller ED, Phillippi JA, Fisher GW, Campbell PG, Walker LM, Weiss LE. Inkjet printing of growth factor concentration gradients and combinatorial arrays immobilized on biologically-relevant substrates. Comb Chem High Throughput Screen 2009;12(6):604–18.
[15] Nelson CM, Tien J. Microstructured extracellular matrices in tissue engineering and development. Curr Opin Biotechnol 2006;17(5):518–23.
[16] Phillippi JA, Miller E, Weiss L, Huard J, Waggoner A, Campbell P. Microenvironments engineered by inkjet bioprinting spatially direct adult stem cells toward muscle- and bone-like subpopulations. Stem Cells 2008;26(1):127–34.
[17] Ruhrberg C, Gerhardt H, Golding M, Watson R, Ioannidou S, Fujisawa H, et al. Spatially restricted patterning cues provided by heparin-binding VEGF-A control blood vessel branching morphogenesis. Genes Dev 2002;16(20):2684–98.
[18] Schultz GS, Wysocki A. Interactions between extracellular matrix and growth factors in wound healing. Wound Repair Regen 2009;17(2):153–62.
[19] Wiradjaja F, DiTommaso T, Smyth I. Basement membranes in development and disease. Birth Defects Res C Embryo Today 2010;90(1):8–31.
[20] de Juan-Pardo EM, Hoang MB, Conboy IM. Geometric control of myogenic cell fate. Int J Nanomedicine 2006;1(2):203–12.
[21] Flaim CJ, Teng D, Chien S, Bhatia SN. Combinatorial signaling microenvironments for studying stem cell fate. Stem Cells Dev 2008;17(1):29–39.
[22] Ilkhanizadeh S, Teixeira AI, Hermanson O. Inkjet printing of macromolecules on hydrogels to steer neural stem cell differentiation. Biomaterials 2007;28(27):3936–43.
[23] Lee YB, Polio S, Lee W, Dai G, Menon L, Carroll RS, et al. Bio-printing of collagen and VEGF-releasing fibrin gel scaffolds for neural stem cell culture. Exp Neurol 2010;223(2):645–52.
[24] Cserjesi P, Brown D, Ligon KL, Lyons GE, Copeland NG, Gilbert DJ, et al. Scleraxis: a basic helix-loop-helix protein that prefigures skeletal formation during mouse embryogenesis. Development 1995;121(4):1099–110.
[25] Scott A, Sampaio A, Abraham T, Duronio C, Underhill TM. Scleraxis expression is coordinately regulated in a murine model of patellar tendon injury. J Orthop Res 2011;29(2):289–96.
[26] Gharaibeh B, Lu A, Tebbets J, Zheng B, Feduska J, Crisan M, et al. Isolation of a slowly adhering cell fraction containing stem cells from murine skeletal muscle by the preplate technique. Nat Protoc 2008;3(9):1501–9.
[27] Qu-Petersen Z, Deasy B, Jankowski R, Ikezawa M, Cummins J, Pruchnic R, et al. Identification of a novel population of muscle stem cells in mice: potential for muscle regeneration. J Cell Biol 2002;157(5):851–64.
[28] Miller E. Inkjet printing of solid-phase growth factor patterns to direct cell fate [Doctor of Philosophy]. Pittsburgh: Carnegie Mellon University; 2007.
[29] Jadlowiec J, Dongell D, Smith J, Conover C, Campbell P. Pregnancy-associated plasma protein-a is involved in matrix mineralization of human adult mesenchymal stem cells and angiogenesis in the chick chorioallontoic membrane. Endocrinology 2005;146(9):3765–72.
[30] Jadlowiec J, Koch H, Zhang X, Campbell PG, Seyedain M, Sfeir C. Phosphophoryn regulates the gene expression and differentiation of NIH3T3, MC3T3-E1, and human mesenchymal stem cells via the integrin/MAPK signaling pathway. J Biol Chem 2004;279(51):53323–30.
[31] Brent AE, Tabin CJ. FGF acts directly on the somitic tendon progenitors through the Ets transcription factors Pea3 and Erm to regulate scleraxis expression. Development 2004;131(16):3885–96.
[32] Springer ML, Ozawa CR, Blau HM. Transient production of alpha-smooth muscle actin by skeletal myoblasts during differentiation in culture and following intramuscular implantation. Cell Motil Cytoskeleton 2002;51(4):177–86.
[33] Clayton RA, Court-Brown CM. The epidemiology of musculoskeletal tendinous and ligamentous injuries. Injury 2008;39(12):1338–44.
[34] Yang PJ, Temenoff JS. Engineering orthopedic tissue interfaces. Tissue Eng Part B Rev 2009;15(2):127–41.
[35] Chan J, O'Donoghue K, Gavina M, Torrente Y, Kennea N, Mehmet H, et al. Galectin-1 induces skeletal muscle differentiation in human fetal mesenchymal stem cells and increases muscle regeneration. Stem Cells 2006;24(8):1879–91.
[36] Elia D, Madhala D, Ardon E, Reshef R, Halevy O. Sonic hedgehog promotes proliferation and differentiation of adult muscle cells: involvement of MAPK/ERK and PI3K/Akt pathways. Biochim Biophys Acta 2007;1773(9):1438–46.
[37] Filigheddu N, Gnocchi VF, Coscia M, Cappelli M, Porporato PE, Taulli R, et al. Ghrelin and des-acyl ghrelin promote differentiation and fusion of C2C12 skeletal muscle cells. Mol Biol Cell 2007;18(3):986–94.
[38] Georgiadis V, Stewart HJ, Pollard HJ, Tavsanoglu Y, Prasad R, Horwood J, et al. Lack of galectin-1 results in defects in myoblast fusion and muscle regeneration. Dev Dyn 2007;236(4):1014–24.
[39] Gros J, Serralbo O, Marcelle C. WNT11 acts as a directional cue to organize the elongation of early muscle fibres. Nature 2009;457(7229):589–93.
[40] Horsley V, Jansen KM, Mills ST, Pavlath GK. IL-4 acts as a myoblast recruitment factor during mammalian muscle growth. Cell 2003;113(4):483–94.
[41] Kim D, Chi S, Lee KH, Rhee S, Kwon YK, Chung CH, et al. Neuregulin stimulates myogenic differentiation in an autocrine manner. J Biol Chem 1999;274(22):15395–400.
[42] Kishioka Y, Thomas M, Wakamatsu J, Hattori A, Sharma M, Kambadur R, et al. Decorin enhances the proliferation and differentiation of myogenic cells through suppressing myostatin activity. J Cell Physiol 2008;215(3):856–67.
[43] Kocamis H, Gulmez N, Aslan S, Nazli M. Follistatin alters myostatin gene expression in C2C12 muscle cells. Acta Vet Hung 2004;52(2):135–41.
[44] Sorci G, Riuzzi F, Arcuri C, Giambanco I, Donato R. Amphoterin stimulates myogenesis and counteracts the antimyogenic factors basic fibroblast growth factor and S100B via RAGE binding. Mol Cell Biol 2004;24(11):4880–94.

[45] Straface G, Aprahamian T, Flex A, Gaetani E, Biscetti F, Smith RC, et al. Sonic hedgehog regulates angiogenesis and myogenesis during post-natal skeletal muscle regeneration. J Cell Mol Med 2009;13(8B):2424–35.
[46] Blau HM, Pavlath GK, Hardeman EC, Chiu CP, Silberstein L, Webster SG, et al. Plasticity of the differentiated state. Science 1985;230(4727): 758–66.
[47] Goichberg P, Geiger B. Direct involvement of N-cadherin-mediated signaling in muscle differentiation. Mol Biol Cell 1998;9(11):3119–31.
[48] Edom-Vovard F, Schuler B, Bonnin MA, Teillet MA, Duprez D. Fgf4 positively regulates scleraxis and tenascin expression in chick limb tendons. Dev Biol 2002;247(2):351–66.
[49] Hoffmann A, Pelled G, Turgeman G, Eberle P, Zilberman Y, Shinar H, et al. Neotendon formation induced by manipulation of the Smad8 signalling pathway in mesenchymal stem cells. J Clin Invest 2006;116(4):940–52.
[50] Wolfman NM, Hattersley G, Cox K, Celeste AJ, Nelson R, Yamaji N, et al. Ectopic induction of tendon and ligament in rats by growth and differentiation factors 5, 6, and 7, members of the TGF-beta gene family. J Clin Invest 1997;100(2):321–30.
[51] Morin R, Kaplan D, Perez-Ramirez B. Bone morphogenetic protein-2 binds as multilayers to a collagen delivery matrix: an equilibrium thermodynamic analysis. Biomacromolecules 2006;7(1):131–8.
[52] Sahni A, Odrljin T, Francis CW. Binding of basic fibroblast growth factor to fibrinogen and fibrin. J Biol Chem 1998;273(13):7554–9.
[53] Collins CA, Olsen I, Zammit PS, Heslop L, Petrie A, Partridge TA, et al. Stem cell function, self-renewal, and behavioral heterogeneity of cells from the adult muscle satellite cell niche. Cell 2005;122(2):289–301.
[54] Quarto N, Wan DC, Longaker MT. Molecular mechanisms of FGF-2 inhibitory activity in the osteogenic context of mouse adipose-derived stem cells (mASCs). Bone 2008;42(6):1040–52.